

# On Degradation Functions and Solution Schemes for a Phase Field Model of Elastic-Plastic Fracture

Timo Noll<sup>1\*</sup>, Charlotte Kuhn<sup>2</sup> and Ralf Müller<sup>1</sup>

## Micro Abstract

A phase field model for elastic-plastic fracture is presented, which is based on an energy functional composed of an elastic energy contribution, a plastic dissipation potential and a fracture energy. The coupling of the mechanical fields with the fracture field is modeled by a degradation function. Numerical simulations are presented, where the choice of the degradation function is investigated and a staggered solution scheme is compared to an also possible monolithic iteration scheme.

<sup>1</sup>Chair of Applied Mechanics, University of Kaiserslautern, Kaiserslautern, Germany

<sup>2</sup>Computational Mechanics, University of Kaiserslautern, Kaiserslautern, Germany

\*Corresponding author: tnoll@rhrk.uni-kl.de

## 1 Introduction

Today, there is a great number of phase field models for brittle fracture originated in the physics as well as in the mechanics community, [2]. A key ingredient for the development of these models from the mechanics community is the variational formulation of brittle fracture proposed by Francfort and Marigo, [4]. For a model considering ductile fracture however, an respective variational formulation is missing, [1]. Nevertheless, in recent years brittle phase field models were extended in order to describe fracture scenarios where crack propagation is affected by plastic deformation. One drawback of most of these models is a rather complex coupling between the crack field and the material laws leading to the necessity to apply staggered finite element solution schemes in order to avoid complicated coupling terms of the monolithic tangent. In this approach a phase field model for quasi-static elastic-plastic fracture is proposed, where the specific coupling of the phase field parameter with the elastic-plastic material law enables a monolithic solution scheme to be employed.

## 2 Model

The model is based upon the free energy density

$$\Psi [\boldsymbol{\varepsilon}(\mathbf{u}), s, \nabla s; \boldsymbol{\varepsilon}^p, \alpha] = g(s) (W_{\text{el}}(\boldsymbol{\varepsilon} - \boldsymbol{\varepsilon}^p) + \Pi_{\text{pl}}(\alpha)) + \psi_{\text{fr}}(s, \nabla s). \quad (1)$$

The elastic energy density  $W_{\text{el}}$  depends on the infinitesimal total strain  $\boldsymbol{\varepsilon}$  and the first internal variable, the plastic strain  $\boldsymbol{\varepsilon}^p$ , since their difference yields the elastic strain. The fracture energy density, which is a function of the crack field  $s$ , where  $s = 1$  indicates intact material, while  $s = 0$  represents fractured material, is denoted  $\psi_{\text{fr}}$ . The plastic dissipation potential

$$\Pi_{\text{pl}} = \alpha \left( \sigma_Y + \frac{1}{2} \alpha H \right) \quad (2)$$

is a quadratic function of the internal variable, representing the accumulated plastic strain  $\alpha$ , in order to account for linear isotropic hardening. The parameters  $H$  and  $\sigma_Y$  represent the

plastic hardening modulus and the initial yield stress, respectively. A degradation function  $g_\beta(s) = \beta(s^3 - s^2) + 3s^2 - 2s^3 + \eta$ , which is equal to 1 for  $s = 1$  and approximately 0 for  $s = 0$  is used to ensure that elastic and plastic contributions of cracked material no longer contribute to the total energy. The parameter  $\beta$  ranges from 0 to 2, where  $\beta = 2$  corresponds to the standard quadratic form, and is adopted from [3]. For stability purposes the parameter  $\eta \ll 1$  is introduced.

The governing equation for the mechanical problem, the balance of linear momentum, and the time dependent Ginzburg-Landau evolution equation for the phase field are

$$\operatorname{div} \boldsymbol{\sigma} = \mathbf{0}, \text{ with } \boldsymbol{\sigma} = \frac{\partial \Psi}{\partial \boldsymbol{\varepsilon}} \quad \text{and} \quad \dot{s} = -M \frac{\delta \Psi}{\delta s}, \quad (3)$$

where  $\boldsymbol{\sigma}$  is the Cauchy stress tensor and  $M$  is a positive kinetic coefficient.

The hardening force  $q$  and the von Mises type yield condition are

$$q = -\frac{\partial \Psi}{\partial \alpha} \quad \text{and} \quad f(\mathbf{s}, \alpha) = \|\mathbf{s}\| + \sqrt{\frac{2}{3}}q = g_\beta(s) \left( \|\mathbf{s}^*\| + \sqrt{\frac{2}{3}}q^* \right) = 0, \quad (4)$$

where  $\mathbf{s}$  denotes the deviatoric part of the Cauchy stress tensor. The quantities marked with  $(\cdot)^*$  indicate undegraded quantities. The evolution laws for the internal variables are

$$\dot{\mathbf{e}}^p = \gamma \frac{\partial f}{\partial \mathbf{s}} = \gamma \frac{\mathbf{s}}{\|\mathbf{s}\|} \quad \text{and} \quad \dot{\alpha} = \gamma \frac{\partial f}{\partial q} = \gamma \sqrt{\frac{2}{3}}, \quad (5)$$

where  $\gamma$  is the absolute value of the slip rate.

### 3 Implementation

From the weak forms of (3), where  $\nabla s \cdot \mathbf{n} = 0$ , with  $\mathbf{n}$  as the outer normal, is assumed on the crack free part of the boundary of the body, a set of discretized nonlinear equations

$$\mathbf{R}(\mathbf{u}, s) = \mathbf{0}, \quad \text{with} \quad \mathbf{u} = \left[ [\mathbf{u}_1]^T, \dots, [\mathbf{u}_N]^T \right]^T \quad \text{and} \quad s = [s_1, \dots, s_N]^T, \quad (6)$$

is yield. The displacement and crack fields in (6) are approximated by their discretized counterparts, where  $\mathbf{u}_I$  and  $s_I$  are the nodal values of the FE discretization. The implicit Euler method is used to approximate the time derivative of the crack field. The residual expression (6) is implemented into the finite element code FEAP as a user element. Healing of cracked material is prevented by fixing nodes to zero, where the crack field has dropped below a prescribed value. The plastic update is determined on element level. The factorization in (4) enables the utilization of an unaltered radial return algorithm [6]. A monolithic scheme as well as a staggered solution scheme can be applied to solve the nonlinear system of equations. Both schemes are outlined in 3.1.

#### 3.1 Solution schemes

In the monolithic solution scheme the residual (6) is solved for all nodal degrees of freedom, three spacial displacements and the crack field, simultaneously. Solutions for the nodal degrees of freedom are iteratively approximated in a single Newton-Raphson loop per timestep. The approximation is considered to be converged if the residual norm meets a prescribed tolerance. In the staggered solution scheme on the other hand, the residual is solved for the three spacial displacements with fixed crack field in a first Newton-Raphson loop and subsequently the crack field is solved for fixed spacial displacements in another Newton-Raphson loop. The solution is considered to be converged if a certain criterion adopted from [2] is met, otherwise the procedure is repeated.

## 4 Numerical Results

A single notched tension probe discretized in  $80 \times 80 \times 1$  brick elements and mounted, such that plane strain conditions apply, serves as a numerical example where the influence of the mobility parameter  $M$  in different hardening scenarios and the performance of the two solution schemes is compared. Therefore, a linear increasing displacement load on the top and bottom edge of the probe is applied. The initial yield stress is chosen  $\bar{\sigma}_Y = 1.0$ . Quantities marked as  $(\bar{\cdot})$ , indicate dimensionless quantities, whereupon the ansatz from [5] used for the transformation. The parameter  $\beta = 0.1$  is chosen for the cubic degradation function. Degradation functions with lower values of  $\beta$  render to be more vulnerable for convergence problems. However, instead a discrepancy between effective and nominal parameters as observed for the standard quadratic function ( $\beta = 2$ ) in [5] is avoided for sufficiently small values of  $\beta$ .

If a high hardening modulus of  $\bar{H} = 0.1$  is chosen, although yield stress has been overcome and plastic strain is present, the driven crack path is straight (see Fig. 1 (a)) and the same as in the purely elastic case. Load displacement curves are independent on the chosen mobility almost identical (see Fig. 1 (b)), whereupon only for  $\bar{M} = 1$  the curve is shifted to slightly higher displacements. If a lower hardening modulus of  $\bar{H} = 0.02$  is chosen, the crack kinks in direction of high plastic deformation (see Fig. 2 (a)). As in the case of the higher hardening modulus, the load displacement behavior is almost independent from the chosen mobility (see Fig. 2 (b)). However, for low mobility  $\bar{M} = 1$  as well as for high mobilities  $\bar{M} = 50$  and  $\bar{M} = 100$  no converged solution was found at the loadings marked with 'x'.

For  $\bar{M} = 10$  and  $\bar{H} = 0.1$  simulations using the staggered scheme are compared to simulations using the monolithic solution scheme in terms of computational performance (see Fig. 3). A constant timestep size was chosen in the simulations using the staggered scheme, while an adaptive timestep algorithm was used in the simulations using the monolithic scheme. The smallest and largest timestep size used with the staggered scheme correspond to the lowest and highest timestep size determined by adaptive time stepping algorithm with the monolithic scheme. Only for the smallest timestep size used with the staggered scheme the simulation is in the same order of magnitude.

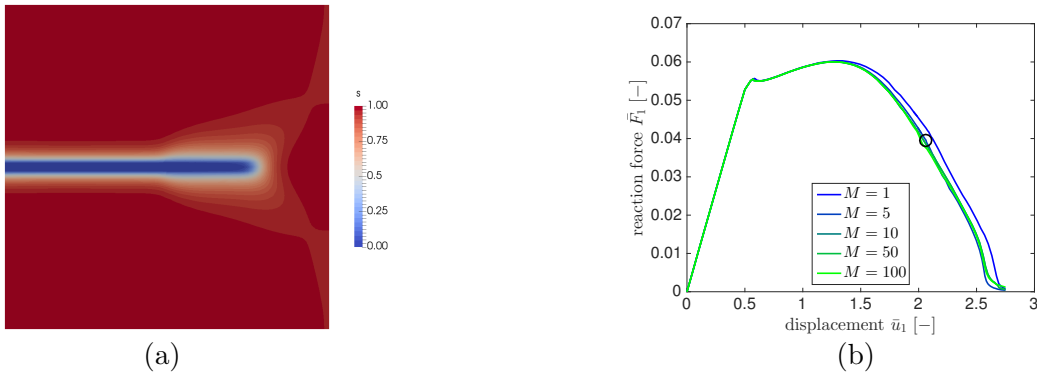


**Figure 1.** Contour plot of the crack field for  $\bar{M} = 5$  and  $\bar{H} = 0.1$  (a) and load displacement curves of the simulations with  $\bar{H} = 0.1$  and varying parameter mobility (b).

## Conclusions

The monolithic solution proves to be more efficient, but reveals stability issues, while the staggered scheme bestows to be very stable, but less efficient. For cubic degradation functions stability issues with monolithic scheme for high and low mobilities in weak hardening scenarios arise.

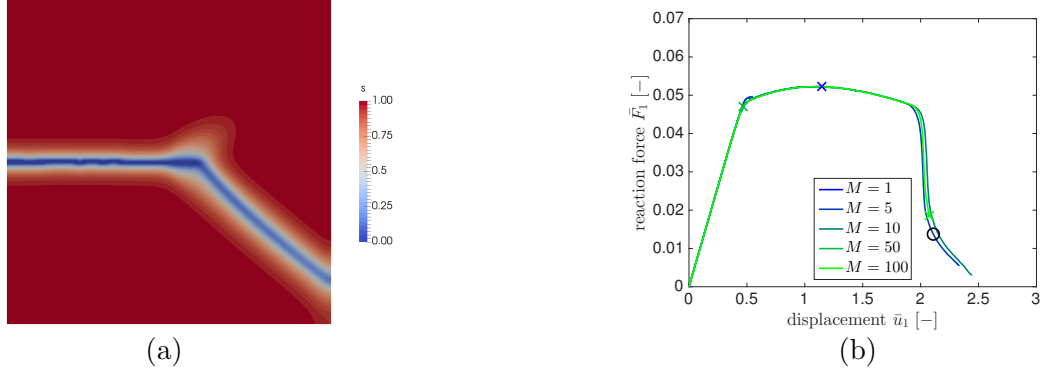


**Figure 2.** Contour plot of the crack field for  $\bar{M} = 5$  and  $\bar{H} = 0.02$  (a) and load displacement curves of the simulations with  $\bar{H} = 0.02$  and varying parameter mobility (b).

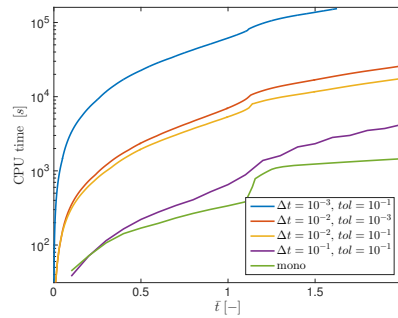


**Figure 3.** Performance curves of monolithic solution scheme with adaptive timestep size and staggered solution scheme with varying constant timestep size and convergence tolerance.

## Acknowledgements

The authors gratefully acknowledge support by the Deutsche Forschungsgemeinschaft in the Priority Program 1748 *Reliable simulation techniques in solid mechanics. Development of non-standard discretization methods, mechanical and mathematical analysis* under the project *Advanced Finite Element Modeling of 3D Crack Propagation by a Phase Field Approach*.

## References

- [1] M. Ambati, T. Gerasimov, and L. De Lorenzis. Phase-field modeling of ductile fracture. 55(5):1017–1040–, 2015.
- [2] M. Ambati, T. Gerasimov, and L. De Lorenzis. A review on phase-field models of brittle fracture and a new fast hybrid formulation. 55(2):383–405–, 2015.
- [3] M. J. Borden, T. J. Hughes, C. M. Landis, A. Anvari, and I. J. Lee. A phase-field formulation for fracture in ductile materials: Finite deformation balance law derivation, plastic degradation, and stress triaxiality effects. *Computer Methods in Applied Mechanics and Engineering*, 312:130–166, Dec. 2016.
- [4] G. Francfort and J.-J. Marigo. Revisiting brittle fracture as an energy minimization problem. *Journal of the Mechanics and Physics of Solids*, 46(8):1319–1342, Aug. 1998.
- [5] C. Kuhn, T. Noll, and R. Mueller. On phase field modeling of ductile fracture. *GAMM-Mitteilungen*, 39(1):35–54, June 2016.
- [6] J. C. Simo and T. Hughes. *Computational Inelasticity*. Springer, New York, 1998.